RESEARCH ARTICLE

D. G. Liebermann · A. Biess · J. Friedman ·
C. C. A. M. Gielen · T. Flash

Intrinsic joint kinematic planning. I: Reassessing the Listing's law constraint in the control of three-dimensional arm movements

Abstract This study tested the validity of the assumption that intrinsic kinematic constraints, such as Listing's law, can account for the geometric features of three-dimensional arm movements. In principle, if the arm joints follow a Listing's constraint, the hand paths may be predicted. Four individuals performed 'extended arm', 'radial', 'frontal plane', and 'random mixed' movements to visual targets to test Listing's law assumption. Three-dimensional rotation vectors of the upper arm and forearm were calculated from three-dimensional marker data. Data fitting techniques were used to test Donders' and Listing's laws. The coefficient values obtained from fitting rotation vectors to the surfaces described by a second-order equation were analyzed. The results showed that the coefficients that represent curvature and twist of the surfaces were often not significantly different from zero, particularly not during randomly mixed and extended arm movements. These coefficients for forearm rotations were larger compared to those for the upper arm segment rotations. The mean thickness of the rotation surfaces ranged between $\approx 1.7°$ and $4.7°$ for the rotation vectors of the upper arm segment and $\approx 2.6°$ and $7.5°$ for those of the forearm. During frontal plane movements, forearm rotations showed large twist scores while upper arm segment rotations showed large curvatures, although the thickness of the surfaces remained low. The curvatures, but not the thicknesses of the surfaces, were larger for large versus small amplitude radial movements. In conclusion, when examining the surfaces obtained for the different movement types, the rotation vectors may lie within manifolds that are anywhere between curved or twisted manifolds. However, a two-dimensional thick surface may roughly represent a global arm constraint. Our findings suggest that Listing's law is implemented for some types of arm movement, such as pointing to targets with the extended arm and during radial reaching movements.

Keywords Planning arm posture · Joint kinematics · Listing's law

D. G. Liebermann (✉)
Department of Physical Therapy, Sackler Faculty of Medicine,
Tel-Aviv University, 69978 Ramat Aviv, Israel
E-mail: dlieberm@post.tau.ac.il
Tel.: +972-3-6405589
Fax: +972-3-6405436

A. Biess · J. Friedman · T. Flash · D. G. Liebermann
Department of Applied Mathematics and Computer Science,
Weizmann Institute of Science, 76100 Rehovot, Israel

C. C. A. M. Gielen
Department of Medical Physics and Biophysics,
University of Nijmegen, 6525 Nijmegen, The Netherlands

Introduction

Purposeful arm movements such as pointing and reaching toward visual targets are highly specialized. We are trained from birth to reach for objects in space, and by early infancy, accurate motion generation is mastered in spite of the computational complexities inherent in such a skill. The fact that more degrees of freedom are available to the arm than the actual ones needed in order to reach and point at a target implies that multiple solutions are available to the motor system for solving this task (the 'redundancy problem'; Bernstein 1967). Bernstein suggested that elementary features of movement and their lawful inter-relationship (i.e., the laws of constraint) may reduce the number of degrees of freedom. Donders' and Listing's laws might be regarded as possible candidates according to which the system may limit the infinite number of options available to move a segment from an initial to a final position. The implications of such laws have been widely investigated with regard to eye rotations.

Donders (1847) observed that for saccadic eye movements performed when the head is fixed, the eye always achieves the same orientation at any position in space regardless of the path taken to reach it or the direction of the saccade. That is, torsion of the eye with

respect to a fixed reference frame depends on the final position, and not on the path followed when reaching that position. The realization of this rule could be achieved by constraining three-dimensional rotation vectors of the eye (relative to an arbitrary reference vector) to lie within a flat two-dimensional map called Listing's plane that maintains a constant direction throughout motion. This is known as Listing's law (Westheimer 1957), which adds a particular specification to Donders' law in that it allows only those postures that can be attained by direct, fixed-axis rotations relative to a primary reference vector.

The projection of unit vectors of rotation onto a flat Listing's plane results in interesting properties. First, Listing's law implies a reduction by one rotational degree of freedom because rotations around all three axes (yaw, tilt, and torsion) can be specified by the coordinates of the rotation vectors projected in the two-dimensional plane. Second, Listing's law is the implementation of a strategy that could minimize the amplitude of rotation if a straight-line path in Listing's plane is assumed. This can be achieved by a rotation from the initial posture of the arm to the final arm configuration about a single axis that is fixed in space (Hepp 1990) under the constraint of Donders' law. This is germane to the arm kinematics modeling approach that will be the focus of the accompanying manuscript.

Evidence in support of a control scheme based on Listing's law has been extensively discussed in the literature concerning eye fixation, saccadic and smooth pursuit eye movements (Tweed and Vilis 1987; Van Opstal 1993; Haslwanter 1995; Crawford and Vilis 1995; Tweed 1999). For saccadic eye movements it was found that the deviations from a flat Listing's plane range between 0.5° and 1.0° in primates and between 1.2° and 1.9° in human subjects (Tweed and Vilis 1990). Therefore, the single-axis rotation hypothesis is fairly well obeyed for the eye. For the arm, the evidence is less conclusive.

A kinematic planning strategy based on an internally represented Listing's plane for the arm has long been suggested as a viable constraint for reducing the computational indeterminacy inherent in this system (Straumann et al. 1991). During a simple task such as pointing with the end-effector, the target can be defined in terms of three spatial coordinates even though four degrees of freedom are available (three for the shoulder and one for the elbow). In this situation, the brain has to make a decision, which in practice means to adopt a constraining rule in order to overcome such indeterminacy. A Listing's law constraint provides a unique solution to this problem.

The application of Listing's law to the intrinsic control of the arm joint rotations has become a focus of research during the last several years (e.g., Hore et al. 1992; Miller et al. 1992; Theeuwen et al. 1993; Gielen et al. 1997; Medendorp et al. 2000; Admiraal et al. 2001). Hore et al. (1992) studied the implementation of Listing's law in a pointing task with an extended arm

rotating about the shoulder, and found that the rotation vectors describing the final angular positions laid in a nearly flat surface for movements within a range of 30° from the center of the workspace. However, for those movements that reached positions at the limits of the workspace (±45°), the surface tended to twist in the direction predicted by a Fick-gimbal system (a fixed horizontal axis, nested inside a frame that allows for rotations around a vertical axis), regardless of the starting position, initial arm posture, visual condition, or body tilt. These initial attempts focused on rotation vectors of the arm describing its posture at the end of the movement. Miller et al. (1992) further expanded this analysis to examine different portions of the movements separately, as well as whole sets of movements during pointing with a fully extended arm. They reported that the deviations (root mean squared distances) from the fitted planes were smaller for rotation vectors obtained within small size workspace regions or within portions of individual movements for the upper arm, when compared to larger strips of the same workspace. However, the orientation of Listing's plane changed systematically. That is, according to their findings one global flat plane could not be used to describe adequately the rotation axes of the upper arm or the forearm segments.

Miller et al. (1992) suggested that the changes in the primary position vectors describing the orientation of the fitted planes could be explained by the curvature of the surfaces found for both the forearm and upper arm segments. Similar results were reported by Gielen et al. (1997) for different movement types, and by Medendorp et al. (2000) who used the rotation vectors obtained from complete sets of continuous movements while subjects kept the elbow joint fixed at different constant angles throughout the movement. Finally, Admiraal et al. (2001) classified movements according to their speed and tested the effects of this factor on the rotation vectors describing the arm configuration during and at the end of the movement.

Following the above research, in the present study we analyzed both fully extended and flexed arm movements based on all the rotation vectors obtained during continuous motion toward visual targets. We included in the analysis sets of radial, frontal, and a mixture of random movements performed throughout the workspace. For these movements we tested whether Donders' and Listing's laws are obeyed throughout the entire movement as well as at the end point. This is relevant for the modeling approach presented in the following manuscript and for our understanding of hand trajectory planning based on the intrinsic arm kinematics. As a preliminary step for including Listing's law as a constraint in a three-dimensional model, we attempt to determine the validity of a Listing's like constraint. For this purpose, the kinematic features of well-defined movements of different types are used in the present investigation in order to examine the nature of the surfaces fitted to the rotation vectors of the forearm and upper arm rotating segments

(Listing's 'displacement planes', Tweed and Vilis 1990). Our approach resembles that of other investigations that tested such assumptions, for example during saccadic eye movements (DeSouza et al. 1997; Tweed 1999).

Materials and methods

Subjects

Four healthy male volunteers completed a series of natural unconstrained arm movements of three different types, performed within a single session. Two participants were 18 years old and the other two were 20 and 32 years old. Movements in this study were carried out using the right arm, and this was the dominant hand for all our subjects. After reading an information sheet, the subjects gave their consent to participate in the experiment as requested by the institutional ethics process. They were free to suspend or drop out from the experiment at any time. Those individuals that agreed to participate were paid after completing the experiment.

Procedures

Subjects sat at a distance of 1 m in front of a projection screen. They were strapped to a chair by appropriate belts that minimized shoulder displacements and fixated the torso throughout the experiment. The height of the chair was adjusted until the right shoulder joint was aligned with a fixed reference point in space. The subjects were then given initial instructions about the experimental task. No further instructions were provided regarding the task or concerning the arm orientation, and therefore, subjects remained naïve about the purpose of the experiments. They were instructed to point toward visual targets that were randomly presented at different locations of the three-dimensional workspace. Targets consisted of 5-cm virtual balls generated and controlled by a computer and back projected on an opaque screen at a frame rate of 71 Hz (via a Barco Ltd projector). All experiments were performed under dimmed lighting conditions, such that subjects were able to see their arm. No additional constraints were imposed upon their movements, and therefore, their performance was expected to resemble natural conditions.

A stereographic method was used to generate a three-dimensional virtual reality display based on a red and a blue presentation of balls shown simultaneously to the right and left eyes, respectively. The two superimposed images were separated and slightly rotated with respect to each other (5°) to generate a visual disparity. For this purpose, subjects wore goggles that filtered out the blue color for the right eye and the red color for the left eye (Kodak filters). The center of the three-dimensional virtual ball was defined as a small sphere that occupied 5% of the ball dimensions and it was visible to the subjects. This was used to standardize the final reaching location among participants. A warm-up period (10 min) was allowed. Visual disparity, image brightness, contrast, and color intensity were individually adjusted in order to enhance the three-dimensional illusion. A series of practice trials were carried out to make the participants familiar with the experimental setup.

Apparatus

Data collection was initiated as the presentation of the virtual images begun. The three-dimensional graphics program delivered a digital signal that served as a trigger for the Optotrak motion tracking system (Northern Digital Ltd). This system was used to obtain segmental kinematics from infrared emitting diodes (IREDs) via two cameras (four sensors, two per camera) that were situated at the ceiling's level (4.20 m height, 3.5 m apart, and 5 m away from the center of the workspace). The system was calibrated at the beginning of each session using a factory-made calibration frame that included 20 IRED markers. The accuracy level of the measurements was within an error of < 0.2 mm. Kinematic data concerning movements of the right shoulder, the upper arm, and the forearm were collected at a sampling rate of 100 Hz. The Cartesian coordinates for each segment were obtained from sets of four IREDs that were attached to the arm via exo-skeletal metal frames. The center of the shoulder frame was placed over the Acromion. A second frame was attached to the distal end of the upper arm and centered over the elbow. This frame was used to measure the rotations of the upper arm relative to the Acromion. A third frame was attached to the forearm, and it was centered over the wrist to allow measuring the rotations of the forearm relative to the upper arm. The wrist was braced to eliminate any rotations of the radio-carpal joint. That is, supination–pronation movements were only possible by rotating the forearm about the radio-ulnar joint.

Experimental protocol

Experimental point-to-point movement data were obtained in sets that included the following movement types:

(1) Extended arm pointing: Nine consecutive sets with 48 movements were performed for each of the nine final target locations (see Fig. 1a). Movements within one set were originated from 24 initial positions but were directed only toward one of the nine possible final targets. Subjects were instructed to point toward the center of a virtual ball, which was projected every 1.5 s on the 1 m × 1 m screen located at a distance of 1 m from the shoulder (i.e., on a frontal plane parallel to the trunk). In this experimental condition, the virtual targets were
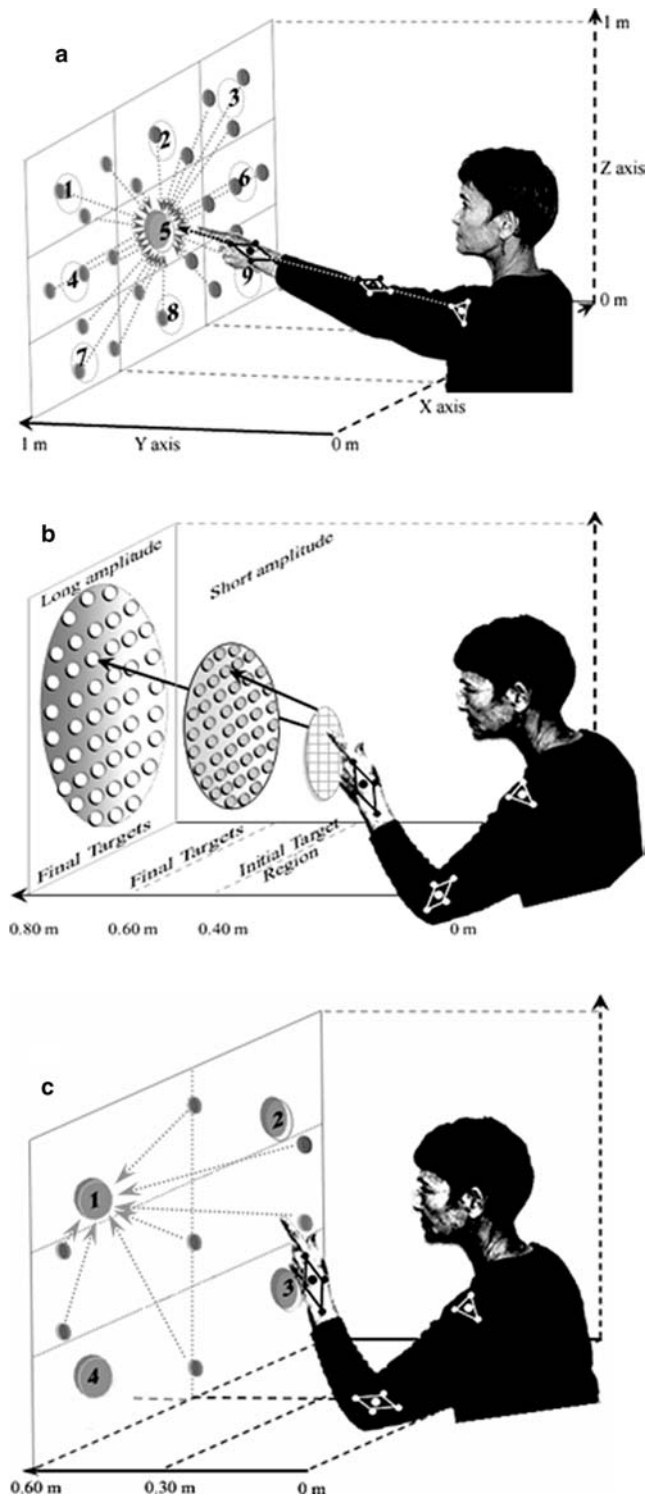
Fig. 1 a–c These illustrations show a 45° view of the experimental setup and the target positions for each of the movement types. The spherical images were back-projected on a 1 m×1 m flat screen that was placed 1 m away from the shoulder. Subjects performed sequences of reaching or pointing movements toward all targets from one or more starting locations. (**a**) Fully extended arm movements: Subjects performed sequences of pointing movements toward one of nine final locations per set (*numbered balls 1–9*) from 24 locations (*unnumbered small balls*). Movements from any location were equally distributed among three horizontal planes at different heights (at 0.3, 0, and −0.3 m relative to the shoulder) and three sagittal planes (*left*, *middle*, *right* at −0.3, 0, and 0.3 m, respectively, from the shoulder). The *geometrical center* of the *screen* was always aligned with the shoulder while the participant pointed toward target position 5, which was the center of the screen. This was the posture where all joint angles were zero. The arm data were aligned with the *x*-axis of a laboratory-fixed reference frame using this configuration. The illustration shows a subject moving from 24 different starting locations that sometimes could overlap with final targets (only to final target 5). The order of the starting targets location was fixed within five blocked sets. (**b**) Radial reaching movements: Subjects moved the hand along the line joining the shoulder and the object. Movements started from the center of the workspace at 0.40 m from the shoulder, and were directed toward 39 final target positions, evenly distributed within the workspace and located at an equal distance from the shoulder, at either 0.60 m (shorter radial movements) or 0.80 m (larger radial movements). A movement started from a center region of the workspace and could end in any of the final targets projected on a curved plane at a fixed distance from the shoulder. (**c**) Frontal plane movements: Subjects performed 12 movements toward virtual balls presented in a frontal plane, aligned in parallel with the frontal plane of the body. Each set consisted of a series of movements that started from six locations in a plane and ended at one final target out of four final target positions contained in the same plane. Two para-frontal planes were used in this experiment, at a distance of 0.30 m and at a distance of 0.60 m relative to the shoulder. The illustration shows the performance of reaching to a final target location (final target 1) from different starting locations in the frontal plane (at 0.6 m from the shoulder) in the same virtual plane

perceived beyond reach, at a distance of 5–10 cm away from the hand along a vector directed with the fully extended arm.

(2) Radial reaching: In this movement type, a set consisted of 78 trials that included shoulder and elbow flexion/extension movements, as illustrated in Fig. 1b. These movements were carried out from a starting position located within an initial target region in the fronto-parallel plane, 0.4 m away from the trunk. For each individual movement, the precise initial hand position was adjusted so that the initial and final targets were in the same direction but at different distances from the shoulder. These movements are referred to in the text as 'radial' movements. The final targets were located either at a distance of 0.6 m (short amplitude trials) or 0.8 m from the shoulder (large-amplitude trials).

(3) Frontal plane reaching: This movement type consisted of sets of movements for which both the initial and final targets were contained within the same frontal plane in parallel to the trunk. Two such fronto-parallel planes at distances of either 0.30 or 0.60 m from the trunk were used (see Fig. 1c), although subjects performed on three different planes in total. Eight different sets of movements (4 in each of the two frontal plane depths) were thus used, with 12 (back and forth) movements each. Each set included sequential reaching movements from six starting locations toward one out of four final targets.

(4) Random movements: A set in this condition included a mixture of 120 pointing and reaching movements performed at different locations within a 1 m × 1 m × 0.80 m workspace randomly chosen from the three previous movement types.

A repeated measures experimental design was used in this study. Every participant performed all sets of movements for five times. Within a set, the order of the movements toward the visual targets remained the same for all five repetitions. The order of the movement types was counterbalanced among sets and participants (e.g., one subject started a testing session with the short-amplitude radial movements while another participant started with the 0.60 m frontal plane movements or with a set of extended arm movements toward final target #1). This was expected to eliminate order-effects and to diminish the effects of fatigue.

Analysis

Raw marker data were collected, stored, and later off-line converted to obtain the three-dimensional Cartesian coordinates. The analyses of the forearm and upper arm data were carried out by implementing an algorithm that used information obtained from at least three visible markers per segment. Missing marker data were reconstructed using a fifth-order polynomial interpolation for portions of the path that showed five or less missing points. The determination of each single trial was based on a time code that assumed a zero velocity at the onset and at the end of a movement within a time-window of 1.5 s. The tangential velocity of a segment was calculated from the X, Y, and Z components of the mean marker data (the segment's centroid).

The rotation vectors in a Listing's plane coordinate system were calculated using the following steps. First, a reference configuration was determined by the mean of the arm configurations extracted from the first 50 frames (500 ms) of each set of trials, while the subject was pointing with the arm fully extended toward the center of the workspace (the initial 'zero configuration' of the arm for all sets of movement). All rotation vectors for a set were then derived with respect to this reference position defined as $\vec{r} = [0, 0, 0]^T$. The shoulder-centered coordinate system was used such that the x-axis was aligned with the arm in the reference position. The z-axis was chosen along the body axis, and the y-axis was defined such that the coordinate system completed a right-hand system. Based on this definition of reference coordinate systems for the upper and forearm segments, rotation vectors $\vec{r}$ for the rotating segments were derived independently for each subject performing the different movement types.

It should be noted that minor changes in the initial position might influence the spatial distribution of the rotation vectors and this could possibly become a source of measurement error. We have carefully validated that the zero arm-configuration at the initial reference position (used to derive the rotation vectors) was the same for all subjects and movement sets. Therefore, we were able to compare different sets of movements.

For any given movement, between a starting position vector in space $\vec{p}_a$ to a final position vector $\vec{p}_b$ we discretized the elapsing time and generated the set of rotation vectors $\vec{r}_i = \vec{r}(t_i)$, where the time t_i is in the interval $[0, t_f]$ and the rotation vectors at the beginning and at the end of the movement are defined by $\vec{r}_a$ and $\vec{r}_b$, leading to $\vec{r}(0) = \vec{r}_a$, $\vec{r}(t_f) = \vec{r}_b$. Rotations with an axis given by $\vec{e}_z = [0, 0, 1]^T$ described left–right rotations. A positive yaw angle corresponded to a rotation toward the left with respect to the zero arm-configuration.

For all movement data in each movement set (see the following paragraph), the rotation vectors $\vec{r}_i = [r_{xi}, r_{yi}, r_{zi}]^T$, $i = 1, ..., n$, were hypothesized to lie within a certain manifold separately defined for the rotations of the upper arm segment and for the forearm segment. The shape of the manifold was determined by estimating the values of the coefficients a, b, c, d, e, and f in the quadratic function $r_x = a + br_y + cr_z + dr_y^2 + er_y r_z + fr_z^2$ fitted to the cloud of the locations representing the tips of the rotation vectors $\vec{r}_i$. The a, b, and c parameters are the respective measures of torsional, vertical, and horizontal deviations relative to the zero arm-configuration (the reference position). The parameters d, e, and f allow for a curvature in the r_y and r_z directions, but only e allows for a twist of the surface. When the values of the coefficients b and c are equal to zero, the manifold describing the rotation vectors is perfectly aligned with the y–z plane but only if the coefficients d, e, and f are also equal to zero. When d, e, and f are zero, the surface would be considered as a completely flat plane as hypothesized by Listing's law. A negative twist score $e = -1$ (when $d = f = 0$) corresponds to rotations in a perfect order-dependent Fick-gimbals system, while a positive twist $e = +1$ corresponds to rotations in reverse order in a perfect Helmholtz system (a fixed vertical axis nested inside a frame that rotates around an horizontal axis).

The best-fitting function was derived by assuming a least mean square criterion, such that the least mean square error function $\sum_i \left(r_{xi} - a - br_{yi} - cr_{zi} - dr_{yi}^2 - er_{yi}r_{zi} - fr_{zi}^2 \right)^2$ was minimized, where $i = 1, ... n$ refers to n data points. As in previous studies, the thickness of distribution of the rotation vectors $\vec{r}_i$ around the fitted manifold (the SD of distance of each $\vec{r}_i$ from the fitted surface) was used to assess to what extent Donders' law is obeyed. The data were analyzed and presented according to different movement sets corresponding to sublevels within the movement type category (see Tables 1, 2). For the extended arm movements, nine different sets of data each (nine final positions), including five repetitions of the same pointing trials, were used. For radial movements two different sets were used, each

with five repetitions. Each radial set corresponded to equal amplitude movements. The analysis was done separately for the large and short amplitude movement sets. Finally, the rotation vectors for frontal plane movements were obtained from eight different sets repeated for five times (four different final positions in one of two possible fronto-parallel planes).

Movements in a particular direction or within small regions were regrouped off-line, and thus, new distributions of rotation vectors were obtained. On these data, further analyses were carried out. The numerical data were stored for statistical analyses using a JMP-2 package (SAS Institute Inc.). Multiple analyses of variance (ANOVAs) were used to determine differences between movement types, directions and rotating segments. The confidence level was set at $P \leq 0.05$ for all analyses.

Results

Listing's law assumes that rotation vectors that describe posture can be mapped onto a flat two-dimensional surface (Westheimer 1957). To address this assumption, the best-fitting Listing's surfaces were calculated and the mean deviations relative to them were calculated for movements directed toward a large number of virtual targets in the three-dimensional workspace. Regardless of the movement task that was being used in the present experiment, zero scores for the coefficients d, e, and f imply that the rotation vector data for a joint would perfectly fit a flat Listing's plane. The coefficients and the SD values around the best-fitting surfaces were used as dependent variables in a series of ANOVAs to assess the flat Listing's plane assumption, and to compare the changes in 'thickness' during movements of different types toward different final target locations.

Figure 2 illustrates results obtained from a mixture of 120 random movements of all types. In this figure, the plots show three-dimensional data of the centroids of the forearm (top panels) and upper arm segments (bottom panels) projected on the three orthogonal planes. The plots shown in Fig. 3 are the distributions of the tip of the rotation vectors of the forearm (top panels) and of the upper arm segments (bottom panels) during the same random mixture of movements.

These examples are representative of the general trend observed for our subjects and provide some initial insights into the shapes of the distributions. The x–y projection is most illustrative (i.e., center panels of Fig. 3) because according to Listing's law, torsion should be zero (i.e., no rotations about x). These data show that even for such a random mixture of movements (different amplitudes and types), the rotation vectors appear to be co-aligned with a planar surface with a thickness of only a few degrees. Note also that the distribution of the upper arm rotation vectors is less scattered than that of the forearm data.

A second-order equation was used to examine more systematically the best-fitting surfaces to our rotations vector data. It should be remembered that the coefficients a, b, and c parameterize the torsion, vertical, and horizontal deviations relative to the reference position, respectively. When b and c are equal to zero, the manifold is perfectly aligned with the y–z frontal plane only if also d, e, and f are equal to zero. The coefficients d, e, and f are measures of the curvature of the plane in the r_y and r_z directions. Therefore, when these coefficients are equal to zero the surface should be completely flat. Values of d and f that are different from zero represent curvature of the plane. If only the coefficient e is different from zero, the surface is twisted.

The values obtained for each of these coefficients are shown in Table 1. The results show that the values of the coefficients b and c were often small and not significantly different from zero. This implied that the manifolds were aligned with the y–z plane.

The coefficients d, e, and f were transformed into absolute values to obtain an estimate of the quantity of curvature and twist of the surfaces. The results show that differences among rotating segments were statistically significant regardless of subject, type of movement, amplitude or directions. The forearm consistently showed larger coefficient scores than the upper arm ($P < 0.05$) in multiple ANOVAs using d, e, or f as the dependent variables. When these scores were equally weighted and combined, the differences did not achieve significance ($t = 3.73$; $P = 0.0537$). Still, the forearm presented slightly higher values and such a trend was maintained throughout the analyses.

Effects of movement types on the coefficients for the forearm segment rotations

As far as curvature of the manifold is concerned (coefficients d and f), the forearm rotations presented scores for d (bent about the y-axis) that were not significantly different for the four movement types. However, when the coefficient f (bent about the z-axis) was used as the dependent variable, the effect was significant ($F_{(3,137)} = 6.034$; $P \leq 0.001$). This effect was attributed to the larger scores observed for the frontal plane movements.

When the score e (i.e., the surface twist) was used as a dependent variable, the analysis of variance also showed a major effect of movement type ($F_{(3,137)} = 5.99$; $P \leq 0.001$). This effect could also be attributed to the significantly larger twist scores obtained for the forearm during frontal plane movements.

Effects of movement types on the coefficients of curvature and twist for upper arm segment rotations

The best-fitting surfaces for the rotation vectors of the upper arm segment could be described as slightly

Table 1 Mean (±SD) coefficients for the surfaces fitted to the rotation vectors of the forearm (A) and the upper arm (B) of four subjects that performed the same sets of movement five times in each of the four movement types, which included different sub-levels

	Levels	a		b		c		d		e		f	
Block A													
Upper	Ext#1	0.03	±0.06	0.02	±0.12	−0.01	±0.18	0.02	±0.80	−0.09	±0.88	*−1.18	±1.02
	Ext#2	0.02	±0.07	0.01	±0.20	0.04	±0.11	0.17	±1.01	−0.25	±0.99	*−0.71	±1.48
	Ext#3	0.03	±0.07	0.04	±0.24	0.05	±0.32	0.32	±1.41	−0.04	±1.08	*−0.94	±1.04
Middle	Ext#4	*0.04	±0.06	0.05	±0.22	0.07	±0.40	−0.24	±0.89	−0.59	±1.65	*1.02	±1.37
	Ext#5	0.01	±0.06	−0.01	±0.19	−0.07	±0.35	0.21	±0.63	*−0.72	±1.27	0.21	±1.47
	Ext#6	0.02	±0.05	0.00	±0.17	−0.03	±0.13	0.32	±0.89	0.13	±1.03	0.11	±0.73
Lower	Ext#7	*0.03	±0.07	−0.02	±0.20	0.02	±0.14	*−0.82	±0.98	−0.21	±1.02	0.29	±0.72
	Ext#8	0.02	±0.08	*0.10	±0.19	*0.09	±0.19	0.51	±1.05	0.36	±1.34	*0.60	±1.02
	Ext#9	0.02	±0.07	*−0.08	±0.15	0.01	±0.23	0.78	±0.93	−0.53	±1.26	0.27	±1.11
Radial	Long	*−0.05	±0.11	−0.07	±0.40	−0.08	±0.20	−0.45	±0.95	0.04	±0.89	−0.10	±0.63
	Short	−0.04	±0.08	0.06	±0.28	0.01	±0.21	−0.08	±0.82	0.42	±1.23	*−0.38	±0.65
0.3 m depth	Front#1	*−0.05	±0.05	−0.08	±0.38	0.11	±0.44	0.68	±1.48	0.13	±1.80	−0.25	±1.44
	Front#2	*−0.04	±0.06	*0.16	±0.30	−0.05	±0.38	*−0.55	±1.13	*1.01	±1.69	−0.36	±1.26
	Front#3	−0.02	±0.07	0.02	±0.45	0.03	±0.57	−0.53	±1.20	0.52	±2.14	0.13	±1.53
	Front#4	−0.03	±0.10	0.02	±0.24	0.05	±0.42	0.19	±0.83	0.36	±1.30	0.30	±1.33
0.6 m depth	Front#5	0.02	±0.10	0.01	±0.25	0.02	±0.50	0.06	±1.12	0.41	±1.39	−0.33	±1.85
	Front#6	0.03	±0.07	−0.11	±0.29	0.10	±0.45	*−0.55	±0.73	0.54	±1.70	−0.19	±2.27
	Front#7	*0.03	±0.07	0.05	±0.42	0.00	±0.34	0.53	±1.53	*0.79	±1.57	−0.25	±1.28
	Front#8	0.02	±0.06	0.01	±0.17	−0.11	±0.32	*0.36	±0.55	0.40	±1.17	−0.17	±1.30
	Mixed	0.04	±0.12	0.02	±0.17	*−0.17	±0.19	0.15	±0.61	0.07	±0.77	−0.25	±0.64
Block B													
Upper	Ext#1	0.02	±0.05	0.00	±0.06	0.00	±0.10	0.32	±0.94	−0.14	±0.69	*−1.01	±0.78
	Ext#2	0.02	±0.05	0.01	±0.07	−0.02	±0.14	0.14	±1.07	0.02	±0.88	*−0.87	±1.01
	Ext#3	0.00	±0.04	0.00	±0.17	−0.08	±0.23	0.37	±1.27	−0.16	±1.21	*−0.84	±0.92
Middle	Ext#4	0.01	±0.04	−0.02	±0.08	0.01	±0.15	−0.28	±0.89	*−0.36	±0.77	*0.50	±1.00
	Ext#5	0.01	±0.05	0.02	±0.09	0.02	±0.08	*0.32	±0.63	−0.22	±0.73	0.05	±0.48
	Ext#6	0.01	±0.04	0.05	±0.12	0.05	±0.15	0.11	±0.60	*0.71	±0.92	−0.11	±0.70
Lower	Ext#7	0.01	±0.05	*0.03	±0.03	0.04	±0.12	*−0.63	±0.95	*0.39	±0.71	*0.55	±0.95
	Ext#8	0.01	±0.05	0.01	±0.14	0.02	±0.11	0.36	±0.85	*0.36	±0.74	0.12	±0.63
	Ext#9	0.00	±0.05	−0.03	±0.13	*0.04	±0.08	0.56	±1.23	−0.23	±0.61	0.20	±0.57
Radial	Long	0.02	±0.06	0.04	±0.18	0.03	±0.09	*−0.68	±0.67	0.30	±0.84	−0.16	±0.45
	Short	*0.05	±0.05	0.04	±0.30	0.01	±0.12	*−0.93	±1.44	0.20	±1.20	−0.13	±0.51
0.3 m depth	Front#1	*0.03	±0.02	0.02	±0.14	0.00	±0.24	*0.37	±0.77	*−1.76	±2.38	0.22	±2.31
	Front#2	*0.01	±0.02	0.01	±0.13	0.01	±0.28	*0.26	±0.49	*0.75	±1.19	*−1.33	±2.47
	Front#3	*0.02	±0.04	*−0.15	±0.23	−0.04	±0.39	0.06	±0.95	−0.95	±2.47	0.10	±2.13
	Front#4	0.00	±0.04	0.04	±0.19	−0.02	±0.30	*0.66	±0.83	0.10	±1.28	*−1.28	±1.79
0.6 m depth	Front#5	0.01	±0.06	0.01	±0.36	−0.02	±0.41	0.28	±0.46	−0.42	±1.58	0.00	±0.98
	Front#6	*−0.03	±0.05	−0.07	±0.32	−0.05	±0.36	0.13	±0.70	−0.07	±1.28	−0.36	±0.92
	Front#7	−0.01	±0.06	*0.24	±0.34	*−0.48	±0.43	*−0.53	±0.53	*1.33	±1.74	*−1.07	±1.45
	Front#8	*−0.03	±0.04	0.05	±0.20	*−0.31	±0.24	0.29	±0.66	0.35	±1.10	*−0.67	±0.75
	Mixed	*0.05	±0.04	0.03	±0.16	0.00	±0.12	−0.20	±0.67	*0.23	±0.38	−0.07	±0.37

Confidence level * ≤ 0.05

curved planes. This was not a consistent observation for all types of movement. However, it contrasted with the twisted manifolds observed for the forearm. The upper arm coefficients introduced as dependent variables in multiple ANOVAs showed significant main effects of movement type when d ($F_{(3,137)} = 10.04$; $P \leq 0.001$) and f ($F_{(3,137)} = 24.61$; $P \leq 0.001$) were used as dependent variables. The former main effect could be attributed to the significantly larger bent of the plane as it was shown from post hoc pairwise comparisons. The comparisons showed that radial movements differ significantly from other movement types ($P \leq 0.001$) in the degree of bent of the plane (i.e., larger values for the coefficient d representing curvature around the y-axis). The latter main effect of movement type (when the f coefficient was used as the dependent variable), could be attributed to differences between frontal plane movements and the other movement types. That is, pairwise comparisons that included frontal plane movements showed significant differences (at $P \leq 0.01$), but extended arm, radial and mixed movement conditions did not differ significantly from each other using f as a basis for the analysis.

Finally, when the coefficient e (the twist score) was used as the dependent variable in an ANOVA (for 'Movement types') the results showed a strong main effect ($F_{(3,137)} = 15.84$; $P \leq 0.001$). As shown previously for the forearm, the e coefficients were significantly larger for frontal plane movements than for other movement types, and certainly larger than those that were obtained for the upper arm rotations. The mixture of all movements performed randomly in all directions showed the lowest twist scores, followed by the extended arm movements.

From the above statistical analyses, it may transpire that a thick two-dimensional Listing's surface may be

Table 2 Mean ($\pm$SD) values (in degrees) of the thickness of the surfaces fitted to the rotation vectors of the forearm (A) and the upper arm (B) during the performance of five repeated sets of movements of four different types, which included different sub-levels

	Levels	S1		S2		S3		S4		Mean	
Block A											
Upper	*Ext#1*	3.54	$\pm$0.60	3.06	$\pm$1.06	4.20	$\pm$1.10	3.14	$\pm$0.78	3.48	$\pm$1.00
	Ext#2	5.05	$\pm$0.77	3.20	$\pm$1.11	4.70	$\pm$1.14	2.91	$\pm$0.42	3.97	$\pm$1.41
	Ext#3	5.05	$\pm$0.94	3.56	$\pm$1.43	5.99	$\pm$0.19	2.73	$\pm$0.42	4.33	$\pm$1.26
Middle	*Ext#4*	6.05	$\pm$0.46	3.79	$\pm$1.72	5.69	$\pm$0.79	3.40	$\pm$0.68	4.73	$\pm$1.20
	Ext#5	4.82	$\pm$0.93	3.66	$\pm$1.38	4.99	$\pm$0.92	2.96	$\pm$0.31	4.11	$\pm$0.90
	Ext#6	5.04	$\pm$1.02	3.02	$\pm$0.87	5.85	$\pm$0.37	3.04	$\pm$0.07	4.24	$\pm$1.09
Lower	*Ext#7*	5.00	$\pm$1.53	2.70	$\pm$0.27	6.03	$\pm$0.67	3.30	$\pm$0.69	4.26	$\pm$0.98
	Ext#8	5.36	$\pm$0.85	3.79	$\pm$1.34	5.74	$\pm$1.03	3.55	$\pm$0.69	4.61	$\pm$1.22
	Ext#9	4.59	$\pm$1.15	3.87	$\pm$0.48	6.38	$\pm$0.17	3.18	$\pm$0.36	4.51	$\pm$1.44
Radial	*Long*	7.72	$\pm$1.07	6.51	$\pm$1.36	7.36	$\pm$0.57	5.11	$\pm$1.75	6.67	$\pm$1.53
	Short	6.45	$\pm$0.48	4.82	$\pm$0.60	6.40	$\pm$0.68	3.90	$\pm$0.87	5.39	$\pm$1.18
0.3 m depth	*Front#1*	5.19	$\pm$1.55	2.64	$\pm$0.68	3.00	$\pm$0.89	3.39	$\pm$0.28	3.55	$\pm$0.28
	Front#2	3.21	$\pm$0.56	1.89	$\pm$0.49	2.21	$\pm$0.68	3.32	$\pm$1.17	2.66	$\pm$0.45
	Front#3	4.26	$\pm$0.86	2.99	$\pm$0.52	2.59	$\pm$0.27	3.39	$\pm$0.66	3.31	$\pm$0.37
	Front#4	3.74	$\pm$0.57	2.30	$\pm$0.31	1.89	$\pm$0.30	2.74	$\pm$0.57	2.67	$\pm$0.49
0.6 m depth	*Front#5*	3.87	$\pm$1.08	2.37	$\pm$0.26	3.67	$\pm$0.64	2.66	$\pm$0.54	3.14	$\pm$0.71
	Front#6	3.40	$\pm$0.68	2.08	$\pm$0.58	3.12	$\pm$0.38	2.82	$\pm$0.49	2.85	$\pm$0.52
	Front#7	4.11	$\pm$0.48	1.93	$\pm$0.59	2.31	$\pm$0.57	2.75	$\pm$0.62	2.78	$\pm$0.91
	Front#8	3.33	$\pm$0.93	1.77	$\pm$0.29	2.49	$\pm$0.77	2.94	$\pm$0.52	2.63	$\pm$0.42
	Mixed	9.04	$\pm$1.10	7.06	$\pm$1.39	8.57	$\pm$1.91	5.38	$\pm$1.27	7.52	$\pm$2.09
Block B											
Upper	*Ext#1*	2.51	$\pm$0.62	2.00	$\pm$0.84	3.91	$\pm$0.99	2.54	$\pm$0.36	2.74	$\pm$1.00
	Ext#2	2.86	$\pm$1.27	2.03	$\pm$0.71	4.97	$\pm$0.68	2.53	$\pm$0.49	3.19	$\pm$1.41
	Ext#3	2.84	$\pm$0.50	2.38	$\pm$0.27	5.09	$\pm$0.69	2.29	$\pm$0.44	3.15	$\pm$1.26
Middle	*Ext#4*	2.69	$\pm$0.20	2.20	$\pm$0.33	4.95	$\pm$0.95	2.72	$\pm$0.37	3.14	$\pm$1.20
	Ext#5	2.81	$\pm$0.77	1.97	$\pm$0.30	4.04	$\pm$0.26	2.41	$\pm$0.31	2.81	$\pm$0.90
	Ext#6	2.67	$\pm$0.80	2.34	$\pm$0.34	4.59	$\pm$0.68	2.32	$\pm$0.16	2.98	$\pm$1.09
Lower	*Ext#7*	3.27	$\pm$0.93	2.05	$\pm$0.19	4.17	$\pm$0.55	2.72	$\pm$0.58	3.05	$\pm$0.98
	Ext#8	2.71	$\pm$0.30	2.37	$\pm$0.52	4.89	$\pm$1.12	2.61	$\pm$0.57	3.14	$\pm$1.22
	Ext#9	2.57	$\pm$0.62	2.54	$\pm$0.38	5.61	$\pm$0.76	2.75	$\pm$0.56	3.37	$\pm$1.44
Radial	*Long*	3.27	$\pm$0.88	2.88	$\pm$0.10	6.37	$\pm$0.24	3.79	$\pm$0.99	4.08	$\pm$1.53
	Short	2.67	$\pm$0.67	2.33	$\pm$0.22	4.93	$\pm$0.81	3.16	$\pm$0.67	3.27	$\pm$1.18
0.3 m depth	*Front#1*	1.77	$\pm$0.30	1.80	$\pm$0.38	1.86	$\pm$0.31	1.77	$\pm$0.23	1.80	$\pm$0.28
	Front#2	2.12	$\pm$0.58	1.66	$\pm$0.39	1.45	$\pm$0.19	1.70	$\pm$0.36	1.73	$\pm$0.45
	Front#3	1.88	$\pm$0.30	2.27	$\pm$0.17	2.19	$\pm$0.48	1.84	$\pm$0.33	2.05	$\pm$0.37
	Front#4	2.50	$\pm$0.32	1.77	$\pm$0.45	2.04	$\pm$0.55	1.67	$\pm$0.14	1.99	$\pm$0.49
0.6 m depth	*Front#5*	2.24	$\pm$0.47	2.58	$\pm$0.61	3.54	$\pm$0.60	2.27	$\pm$0.24	2.66	$\pm$0.71
	Front#6	2.24	$\pm$0.47	1.87	$\pm$0.15	2.89	$\pm$0.34	2.42	$\pm$0.51	2.35	$\pm$0.52
	Front#7	2.18	$\pm$0.73	1.97	$\pm$0.23	3.41	$\pm$1.10	2.01	$\pm$0.60	2.39	$\pm$0.91
	Front#8	1.84	$\pm$0.36	1.70	$\pm$0.14	2.53	$\pm$0.39	1.92	$\pm$0.14	2.00	$\pm$0.42
	Mixed	3.66	$\pm$1.03	3.20	$\pm$0.32	7.64	$\pm$1.67	4.43	$\pm$1.35	4.73	$\pm$2.09

representative of a general constraint imposed on the upper arm joint rotations during reaching and pointing. In extended arm movements, this was a typical finding suggesting that a planar description may be particularly relevant for rotations of the shoulder joint. In radial movements, the plane was slightly curved, but not consistently so for all subjects. Major twists and curvatures were found for frontal plane movements. Mixed movements, randomly mixed among the different directions within the workspace, may be represented by a thick two-dimensional description. The coefficients *d*, *e*, and *f* in this condition (Table 1a-b, last row of A and B parts) were relatively small and mostly not significantly different from zero.

The mixed movement condition included extended arm, radial and frontal plane movements. Therefore, a manifold representing such a mixture of movements

could be assumed as an expression of a general constraint imposed upon the rotation vectors of the arm.

In order to visualize such a general description for the upper arm and forearm postures, a series of quadratic surfaces were obtained using the values of the coefficients that resulted from inserting the rotation vector data $(\vec{r}_i)$ of 120 consecutive trials into the equation shown in Sect. 'Analysis'. Since each subject performed five sets of such a mixture of 120 trials, we calculated five surfaces per subject. The resulting surfaces are shown in Fig. 4 for the forearm rotations and in Fig. 5 for the upper arm rotations.

Considering that the present experimental task included the performance of mixed movements randomized among the three movement types (extended arm, radial and frontal plane movements) and many different movement directions within our workspace, the results

Fig. 2 The figure shows a general example of one set of 120 three-dimensional point-to-point movements performed between virtual targets located at random positions (from a pool of the target positions) in three different movement types investigated in the present study. These plots show path coordinates (in mm) of the geometrical means (the centroids) of the four wrist and the four elbow markers (top and bottom rows, respectively), projected on three orthogonal planes (from left to right: *z–y* front, *z–x* side, and *y–x* top views)
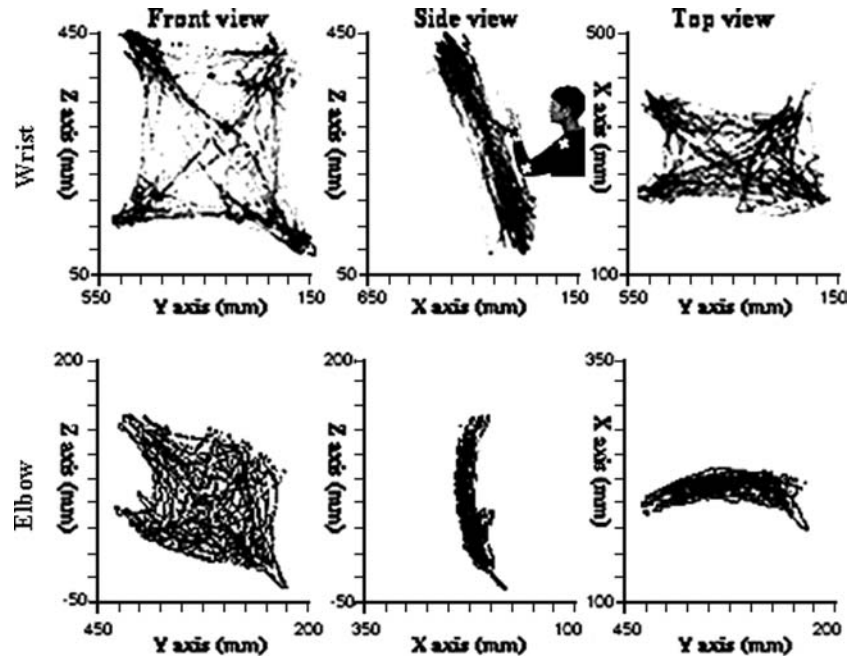
may be representative of a global constraint. Such a constraint that is imposed on the arm joint rotations and in particular on the rotations of the shoulder joint may be represented by a two-dimensional surface.

Donders' law for the forearm and upper arm segments

Donders' law states that the torsion component with respect to a fixed reference frame is predetermined by the
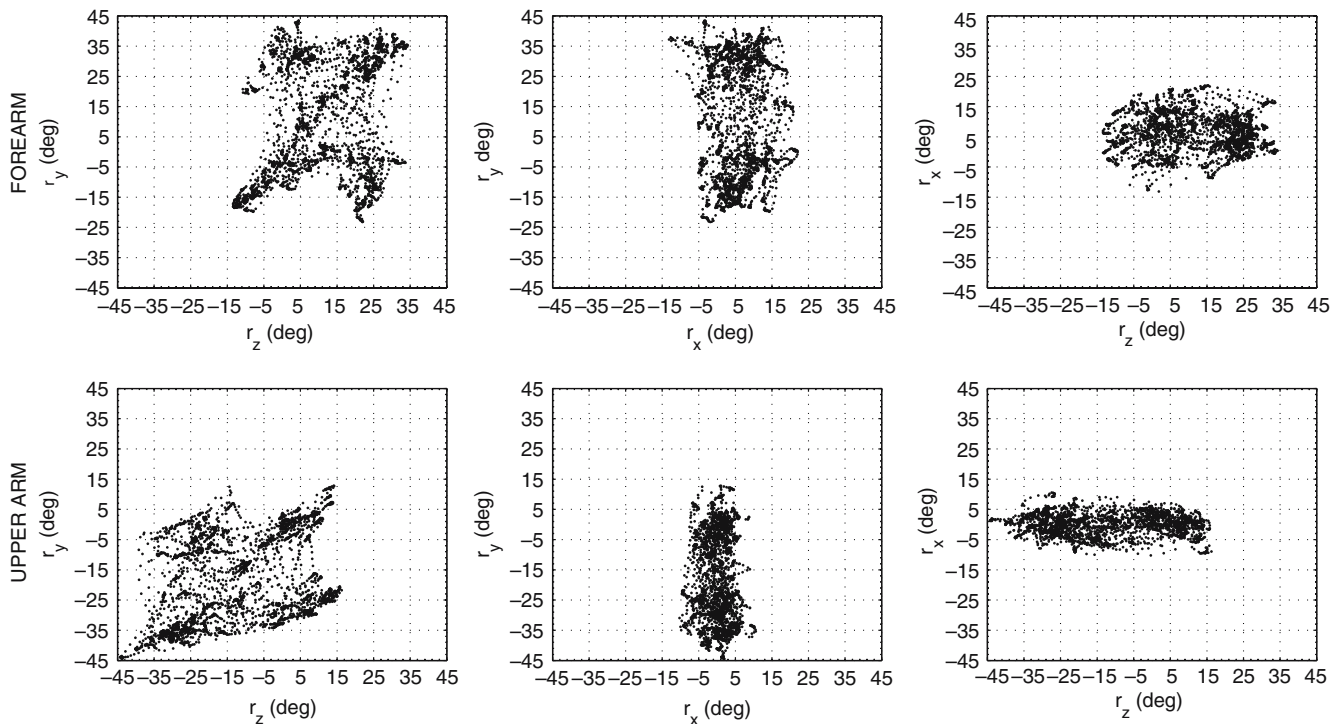
Fig. 3 Three-dimensional rotation vectors of the forearm and upper arm segments (*top and bottom panels*, respectively) are projected on three orthogonal planes. The *X*-axis of rotation describes the torsion component of the rotation vectors (expressed in degrees). The distribution of the tips of the rotation vectors in these plots correspond to the arm segment trajectories shown in

Fig. 2. The possibility that a two-dimensional Listing's constraint may be used for the arm segment rotations transpires from these data examples (particularly, for the upper arm, in the *bottom row*), which include a mixture of reaching and pointing movements performed toward visual targets presented randomly at different workspace locations
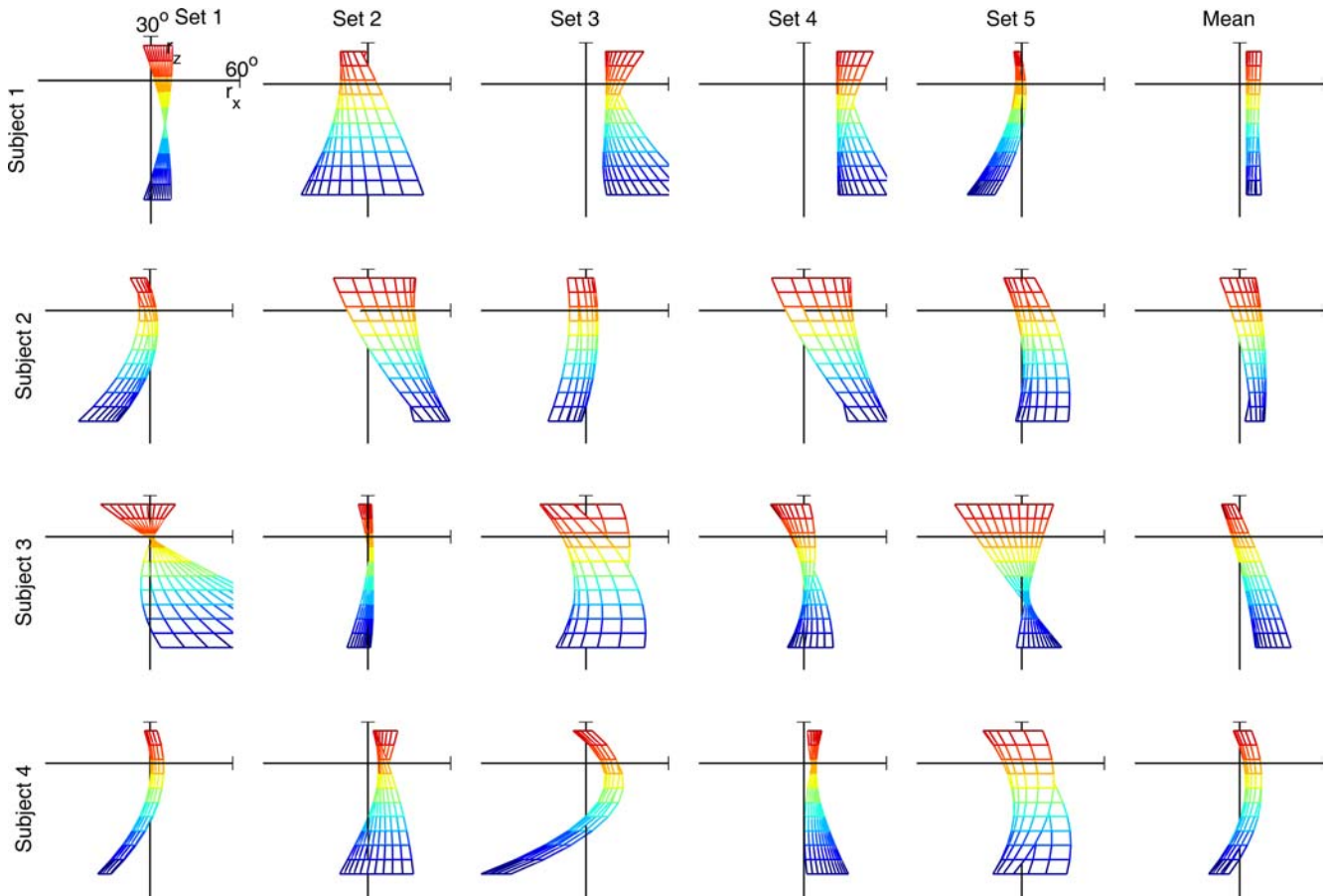
Fig. 4 Surface best-fits of forearm segment rotations of subjects #1–4 (rows #1–4) repeated five times in sets of $N = 120$ movements (columns #1–5 from left to right). The surfaces were generated from the coefficients of the second-order equation $r_x = a + br_y + cr_z + dr_y^2 + er_yr_z + fr_z^2$ applied on the tip of the arm rotation vectors that resulted from the movements in each set of randomly mixed trials. The last column of plots (column #6) presents the mean surfaces for each subject, which resulted from averaging the coefficients obtained for the different sets. Each plot shows a view orthogonal to the XZ-rotation plane, which enables to visualize the shapes of the best-fitting surfaces. The axes representing the size of the fit to the rotation vectors are expressed in degrees. The centers of origin and the sizes of the distributions of the rotation vectors in space slightly differed from each other

final position and does not depend on the path followed by the hand for reaching that position. Listing's law only limits Donders' law to those positions that can be attained by a direct rotation from a primary reference vector. This is done by constraining the three-dimensional rotation vectors to lie within a Listing's surface.

Based on the results previously shown, it could be argued that a significant portion of our rotation vector data may be contained within a two-dimensional surface with a thickness of a few degrees. As a test of the validity of Donders' law under the constraint of a Listing's law, we assessed the thicknesses of the Listing's surfaces that best fitted the rotation vectors obtained for the four subjects. For this purpose, we calculated the SD of the distance from completely flat or curved surfaces.

A three-way mixed design ANOVA (four 'Movement types' × two 'Segments' × two 'Manifolds') was carried out on the SD values (in degrees). The results of this analysis showed that the thickness of the curved surfaces for either joint or movement types was smaller than that for a completely flat plane assumption ($F_{(1,296)} = 23.77$; $P < 0.001$). However, on average the values were similar (for planar constraint the mean was 3.63°, while for curved and twisted surfaces the mean was 3.37°).

A question of concern is whether such a significant reduction in the variance around a quadratic surface leads to a better model for explaining the orientations adopted by the arm, or if such a reduction in variance is simply a byproduct of the additional terms used in the equation. In fact, the quadratic model resulted in a relatively small improvement as compared to the linear model. This improvement ranged between 0.0 and 0.21° for the upper arm and 0.22–0.6° for the forearm. That is, within the resolution of the current modeling efforts, the use of additional free parameters in the fitting equation cannot explain meaningfully the variance around a planar best-fit. A variance of 3.6° around a flat plane accounts for an error of less than 2% in describing the orientation of the human arm, which can reach torsion values of > 180°. Therefore, the assumption of a Listing's constraint as described by the planar fit might be reasonable.
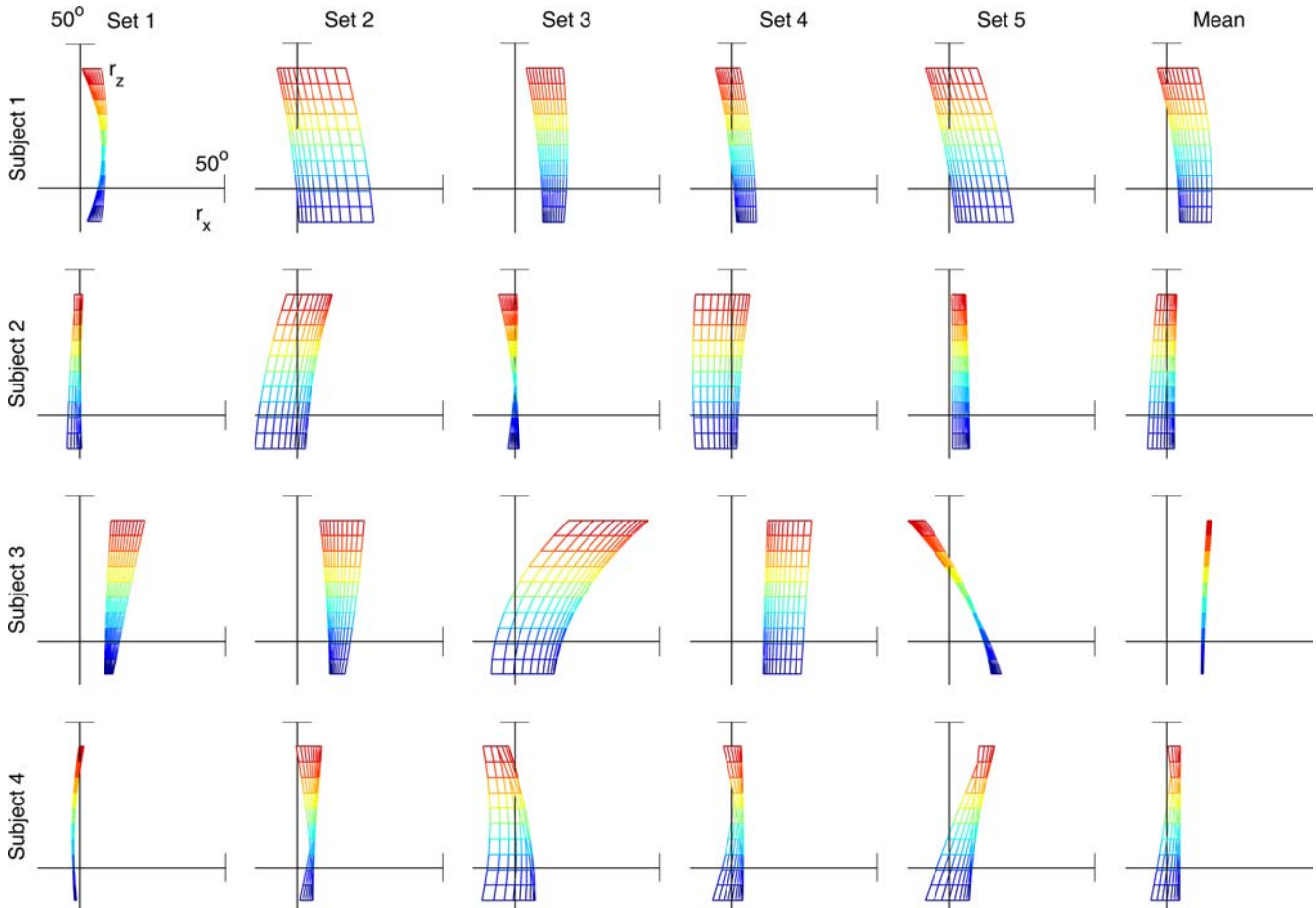
Fig. 5 Surface best-fits of upper arm segment rotations of subjects #1–4 (rows #1–4) repeated five times in sets of $N = 120$ movements (columns #1–5 from left to right; mean surfaces in the last column). The surfaces for the upper arm were also generated from the coefficients of the second-order equation $r_x = a + br_y + cr_z + dr_y^2 + er_yr_z + fr_z^2$ applied on the tip of the rotation vectors (as for the forearm). Visual inspection of these surface shows that the thickness and shape of the best-fitting surfaces for the upper arm are closer to a two-dimensional manifold. Deviations are expressed in degrees

The mean values for the thickness of the surfaces obtained for the different movement types are shown in Table 2.

These findings show relatively small SD values suggesting that arm rotations during three-dimensional movements may follow Donders' law. A two-way mixed design ANOVA (four 'Movement types' × two 'Segments') with repeated measures on the first factor was carried out using SD as the dependent variable. The results showed that all main effects were significant. Since all movement type categories included movements toward the same target positions, any differences in the thicknesses of the surfaces could not be attributed exclusively to differences in final locations. Movement type appeared to exert a larger influence on the suitability of Donders' law to our data ($F_{(1,3)} = 169.9$; $P \leq 0.001$). The 'Segments' main effect ($F_{(1,1)} = 204.4$; $P \leq 0.001$) showed that the forearm and the upper arm segments significantly differed, as it was already found for the shape of the surfaces.

Forearm rotation vectors resulted in thicker surfaces as compared to those surfaces fitted to the rotation vectors obtained for the upper arm. The interaction between segments and types of movement was also significant ($F_{(1,3)} = 12.1$; $P \leq 0.001$). The surface thickness was relatively small for the upper arm rotations regardless of movement type, and significantly larger for the forearm rotations, particularly in the radial and mixed movements. These differences between movement types and rotating segments are illustrated in Fig. 6.

As it stems from the present results, Donders' law during hand movements toward visual targets may be implemented for the arm as a whole, but differently when the two arm segments are separately considered. The findings indicate that the upper arm may be constrained to follow Donders' law regardless of the movement types and of the paths taken to reach a final target. However, this does not appear to be the case for the control of the forearm orientation.

Fig. 6 This plot shows differences in the thickness (SD in degrees) of the distributions of rotation vectors around best-fitting Listing's surfaces for the forearm and upper arm segments when the subjects performed pointing at targets using different types of movement. Mean values (in degrees) are shown inside the columns, while the SD values around the mean thickness are shown near and above the error bars, at the top of each column
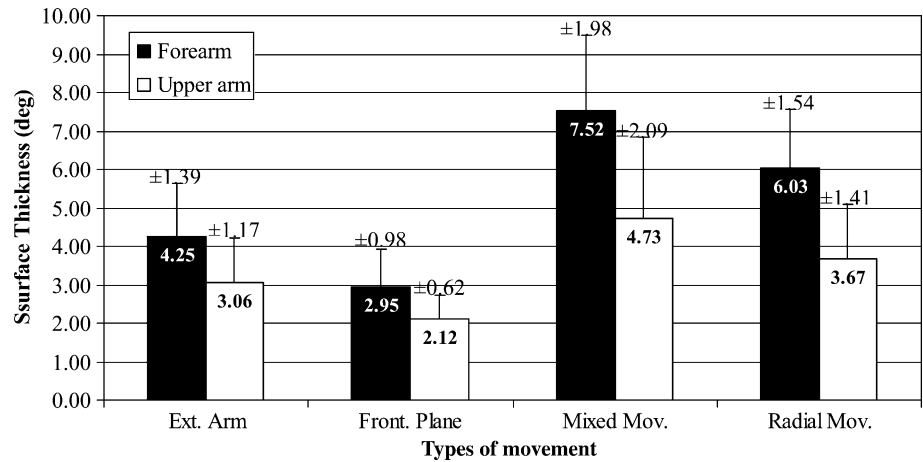
Moving within small sub-regions of the workspace

The following analyses were carried out to explore the effects of moving locally within smaller workspace regions on Donders' law. Nine small spaces were defined for this purpose (see the division into these smaller regions in Fig. 1a). Movements that were carried out within any of the small regions of size 0.3 m × 0.3 m were used for the analysis. ANOVAs yielded significant major effects for all factors. A strong effect was found for 'Workspace region' ($F_{(8,171)} = 22.94$; $P < 0.001$) suggesting that the implementation of Donders' law for movements toward targets concentrated within different local regions was not the same. The analyses showed that the larger scatter was obtained for movements toward targets located in the lower-left region (e.g., sub-region #7 in Fig. 1a).

To further study the effects of moving within different workspace regions on the fit to Donders' law, data were grouped over horizontal strips of movements (upper strip: movements only within sub-regions #1–3; middle strip: movements only within sub-regions #4–6; and lower strip: movements only within sub-regions #7–9). Tukey-HSD post hoc comparisons showed that the fit to the surfaces for each block of movements was different.

Movements performed within the upper horizontal strip differed significantly from those performed within the middle ($t = 4.62$; $P < 0.001$) and lower strips ($t = 3.94$; $P < 0.001$), and movements carried out within the middle horizontal strip significantly differed from movements performed within the lower horizontal strip ($t = 4.98$; $P < 0.001$). That is, the thickness of the surfaces fitted to the rotation vectors of both forearm and upper arm segments decreased in a top–down direction.

When the data were blocked in vertical strips (right strip: movements only within sub-regions #3, #6, and #9; central strip: movements within sub-regions #2, #5, and #8; and left strip: movements within sub-regions #1, #4, and #7), the results also showed a significant effect of the workspace region ($P < 0.001$). However, no clear trend was evident for such vertically grouped movements.

Moving only toward targets within the central vertical column did not differ significantly from movements within the left vertical column, although on average the rotation vectors obtained from arm movements along the central vertical strip were more closely aligned with Listing's surface.

Finally, movements carried out within the right vertical column differed from movements performed within the central strip ($t = 3.34$; $P < 0.001$).

Donders' law during pointing at different locations in the workspace

As a final attempt to test the validity of Donders' law, we assessed the thickness of the Listing's surfaces during pointing with a fully extended arm, separately toward nine different final target positions starting from the same 24 initial locations. This was done separately for five times for each of the four subjects. Analyses were performed in order to examine whether pointing to any of these final target locations from different initial positions had an effect on the thickness of the upper arm Listing's planes. A one-way ANOVA (nine levels of the 'Target location' factor) showed that the amount of scatter of the rotation vectors was affected by the target location ($F_{(8,171)} = 3.02$; $P \leq 0.005$). Tukey-HSD post hoc analyses showed that such an effect could be attributed to the performance of movements toward the lower-left corner (target #7). Movements toward that position showed a larger variance around the best-fitting surface as compared to movements carried out toward other final positions.

This effect was the same regardless of whether the fitted surface was flat, bent or twisted. Movements toward the center of the workspace (target #5) presented somewhat smaller deviations. A significant 'Subject × Target location' interaction was observed ($F_{(24,129)} = 2.09$; $P \leq 0.005$).

Discussion

The goal of this study was to test the general validity of Listing's law as a constraint for the rotations of the joints of the arm during the performance of tasks such as reaching and pointing toward visual targets. Donders' law was also investigated under the constraint of Listing's law in different movement conditions.

In the last few years, several authors have tested these laws for the upper limb segments. We attempted to expand beyond previous experimental studies by including large sets of functionally relevant movements of different types, performed either separately or in a random mixture.

Our results showed that when a surface was fitted to the arm rotation vectors, the coefficients of curvature and twist were not (and could never be) exactly zero regardless of the movement type. At first glance, this may imply that the flat Listing's plane assumption in its strictest sense is violated. However, for the upper arm we often observed that the coefficients d, e, and f (allowing for curvature and twist of the surfaces) were not significantly different from zero. That is, even when some degree of curvature or twist could have been fitted to the rotation vectors of the upper arm, we found that a two-dimensional Listing's constraint might be considered as a rough but good first-order approximation. Donders' law and a two-dimensional Listing' constraint might be global and might be considered as a general strategy of control. Deviations from such a general plan may depend on several factors. The type of movement being performed and the functional role played by the different arm segments are among such factors.

Significantly, during the random mixed sets of movements the SD around the best-fitted surface for the upper arm was small (only 4.73° on average), suggesting that Donders' law might have been obeyed. In addition, the surfaces found for those movement trials were close to being two-dimensional (Figs. 3, 4), suggesting that Listing's law was also followed.

Listing's law for different body segments under different task demands and movement types

Throughout Sect. 'Results', we have reported that the forearm and the upper arm segments significantly differ from each other, regardless of the type or the direction of movement. Forearm rotation vectors often fitted curved or twisted surfaces, and presented significantly larger variance around the best-fits. On the other hand, the upper arm segment adopted postures that fitted closer to a plane and presented thickness values that were significantly lower than the values found for the forearm (see Tables 1, 2).

Theeuwen et al. (1993) studied the possibility of an independent control of different limb segments during pointing and reaching, and concluded that the rotation vectors of the head and the shoulder fit two curved rotation surfaces that are different and uncorrelated. This suggests that the two segments are controlled independently even though the same constraint is applied to both. In the same vein, Medendorp et al. (2000) showed independence in the implementation of Listing's law for the eyes versus the arms, and even within the arm joints (i.e., an independent control of the shoulder, elbow, and wrist joints).

In fact, the different joints might be functionally dissociated such that either each segment becomes an independent component or, if necessary, one more component of a functional unit. Such a 'flexible' control strategy is carried out by imposing additional coupling rules upon the joints. Timing constraints between joints depend on the task goal. The findings reported by Ceylan et al. (2000) for rotations of the eyes and the head suggest such a possibility. Normally, eye and head movements can be controlled independently, but a change in the task such as allowing only visual input by looking toward a target through pinhole goggles causes the head to behave like the eye. Consequently, the head obeys Listing's law as the eyes would have obeyed it (Ceylan et al. 2000).

Further evidence comes from clinical observations. In severe torticollis, the head remains fixed in an extreme position relative to the trunk. Therefore, the eye and head behave as a unit and tend to rotate about a common single axis (as if Listing's law were equally used for both; Medendorp et al. 1999).

More compelling evidence comes from the study of Marotta et al. (2003). These authors reported that Donders' and Listing's laws may be relevant for the orientation of the hand at the end of reaching and grasping movements to pre-oriented objects. For such task, both the upper arm and the forearm obey Donders' law but the upper arm follows Donders' law more closely than the forearm, similarly to our findings. Their evidence shows that orientation of the upper arm depends on the forearm orientation, and this in turn depends on the orientation of the object to be grasped. A different Donders' law constraint was found for each endpoint object orientation, although the object was placed in different locations in the workspace. The shapes of Donders' surfaces for each orientation were found to be relatively flat. Marotta et al. (2003) found that both the upper arm and the forearm obey these constraints. The upper arm was observed to follow Donders' law more closely than the forearm. However, they looked for evidence of a Donders' law constraint only at the endpoint and not during the hand transport. At the end of the movements, they report a linear relation between changes in orientation of the arm segments with respect to each other and with respect to the orientation of the object in space.

Our results also suggest that the brain may control joint motion using Donders' law but under the limitations of a global Listing's surface that acts as a constraint during the arm movement to a target. Its

implementation may be dependent on the requirements of the movement task being performed.

Suitability of Listing's law for different target configurations in space

Our analyses showed that rotation vectors for movements performed at eye level (regardless of azimuth) and for movements performed over the right vertical side ipsilateral to the pointing arm (regardless of target height), laid significantly closer to a Listing's surface. The largest variance around the fitted surfaces was observed during movements directed toward the lower-left corner (target position #7, see Fig. 1a).

This may appear to be in contrast with the results reported by Soechting et al. (1995). These authors tested if the final postures are constrained by Donders' law or by the intent to minimize peak kinetic energy. Soechting et al. (1995) found that only movements near target locations that resemble our target position #7 complied with Donders' law. Our results show that the deviations from the best-fitting surface increase during pointing toward target position #7.

There is no contradiction between those previous findings and ours. Soechting et al. (1995) studied arm postures adopted during pointing to real targets and tested the variance around the torsion component *at the end of the movements* toward the lower-left corner of the workspace. In our experiments, the rotation vectors of the arm were collected *throughout the entire movements* toward the lower-left corner (and the other positions).

Different manifolds could describe our spatial arrangement of arm rotation vectors during ongoing movements, although only a completely flat Listing's plane would have implied that Donders' law is uniquely obeyed under the constraint of Listing's law, either during or at the end of such movements. We have not obtained such flat planes from our data but found support for Donders' law regardless of the shape of the quadratic surfaces that we have allowed for (relatively low SD values around the best-fitting surfaces). The only exception was for movements toward the lower-left region.

We may speculate about additional reasons for the discrepancies between Soechting et al.'s (1995) and our results, and attribute these differences to variations in the experimental tasks. In the study by Soechting et al. (1995), the subjects used a pointer in order to point at real targets, while our subjects used the index finger to point at virtual targets. In addition, in our experiments the lower-left corner was at a position closer to the biomechanical limits of the right arm, while in Soechting et al.'s study (1995) subjects probably never reached such limits.

In the next paragraphs, other findings are discussed in light of the existing literature on Donders' and Listing's laws in the control of arm movements. Effects that are more specific will be dealt with next, with an emphasis on the functional significance of the task and the possible effects of arm dynamics during movement execution.

How do movement dynamics during execution affect a kinematic plan based on Listing's law?

While a Listing's constraint may be a basis for the kinematic planning of arm movements, its implementation might not be as evident because of the possible influence of arm dynamics on the movement outcome. In our study, at least two major factors may have led to the magnification or reduction of the effects of limb dynamics on the observed kinematics: the amplitudes and the types of movement being generated.

With regard to the first factor, we observed a systematic increase in the variance around the Listing's surface and larger curvature and twist scores during movements with large versus small amplitudes. Such deterioration in the fit to a Listing's surface has been shown for eye movements when the amplitude of the eye rotations is increased even though dynamic effects for the eye are not large (Glenn and Vilis 1992). Therefore, dynamics only cannot explain deviations from Listing's law with increases in movement amplitudes. In fact, Mitra and Turvey (2004) have shown that neither moving a pre-loaded hand to different target locations nor moving at increasing speeds to those targets did affect the degree to which Listing's law is obeyed. As it stems from our arm movement experiments, dynamic effects may have contributed to the accumulation of errors at execution of an already structured plan based on Listing's law. An expression of such an error is the increase in the thickness around the best-fitting surfaces with changes in movement amplitude.

Movement type is the second factor that has influenced the fit to Listing's surfaces. According to our results, deviations from Listing's surfaces were generally small and the surfaces were close to being two-dimensional as is implicit in Listing's law, with the exception of movements in the frontal plane. The rotation vectors for this type of movement tended to fit twisted surfaces. During reaching for targets within a frontal plane, subjects tended to drop the elbow down in the direction of gravity. Therefore, the rotation vectors may have been constrained to follow the Fick-gimbals strategy that allows for the minimization of kinetic energy (Hore et al. 1992; Soechting et al. 1995).

Dynamic interactions can account for errors at execution

Inter-segmental dynamic interactions may play a significant role in determining to what extent dynamics exert an effect on movement kinematics at the execution stage. These interactions change as a function of the movement task.

Hollerbach and Flash (1982) argued that straight-line hand paths reflect either computation of or compensation for the effects of inertial, centripetal, and Coriolis interactive forces that operate during motor execution. In the absence of a proper compensation for dynamic interactions, one would not have expected to observe straight hand paths as reported for point-to-point movements in the horizontal plane (Morasso 1981). In the analysis of interaction torques, Hollerbach and Flash (1982) showed that during straight-line radial reaching, Coriolis and centripetal torques about the shoulder joint cancel each other out while the elbow's inertial torque still operates at the shoulder joint. On the other hand, during whipping movements, the centripetal and Coriolis velocity-dependent interaction torques that operate at the shoulder joint are not cancelled out.

Although in our study radial reaching movements are three-dimensional, such movements were mechanically similar to the two-dimensional movements studied in Hollerbach and Flash (1982). Similarly, the frontal plane movements studied here were in part quite similar to the whipping two-dimensional movements studied in Hollerbach and Flash (1982). Therefore, the influence of the interaction torques at the shoulder and elbow joints should be taken into consideration here as a partial explanation for the deviations observed from a Listing's constraint, certainly during frontal plane as well as radial movements.

Validity of Listing's constraint as a general working assumption

It was shown in earlier studies that deviations from a Listing's plane are larger for the arm than for the eyes (Tweed and Vilis 1990). It has also been argued that rotation vectors about the shoulder and the wrist joints do not obey a flat Listing's plane assumption (Hore et al. 1992). Considering the mechanical and functional differences between the eye and the arm, the reported discrepancies are not surprising. Other authors have indeed doubted the validity of a flat Listing's plane constraint during reaching and pointing movements, and have argued that arm rotation vectors might be better considered to lie within twisted or curved planes.

Theeuwen et al. (1993) found fits with twist coefficients between 0 and −1 during pointing at visual targets (with the hand or with the nose) suggesting that the rotation surfaces representing the head, arm, and hand were twisted (a Fick-gimbals system of rotations). Gielen et al. (1997) and more recently Medendorp et al. (2000) have concluded that the distribution of the rotation vectors of the arm segments may be better described by a curved surface. They based their conclusion on the coefficients of twist or curvature of the regression equations computed for rotation vectors. Our experimental observations showed also that the d, e, and f coefficients of the second-order equation in the different conditions were seldom significantly different from zero

(see Table 1), and therefore, a flat Listing's plane may be used. We also included large sets of randomly mixed natural reaching and pointing movements directed toward all target locations within our workspace. This condition allowed for the calculation of distributions of rotation vectors that may be representative of a more generalized constraint imposed upon the arm joints, as hypothesized earlier by Miller et al. (1992). An advantage of such general constraint is the simplification of joint orientation control by using one common fixed-oriented reference.

During the mixture of movements toward different random target locations, we have found that the coefficients of curvature and twist for our data were small, particularly for the upper arm (compare the mean d, e, and f coefficients in the mixed condition in Table 1). In addition, the mean thickness of the surfaces for such sets was also relatively small (compare the bottom rows in parts A and B of Table 2). The question of whether a two-dimensional Listing's constraint is a reasonable assumption (even if some degree of curvature or twist might be present) for the surfaces fitted to the data can be answered from looking at Figs. 3 and 4. The thickness of these surfaces was on average small, and thus, the potential contribution of the curvature and twist to the accuracy of a two-dimensional description appears negligible for arm joint rotations.

Donders' and Listing's laws might describe fundamental constraints which are imposed on the planning of arm postures. They could be implemented for a single arm joint or for multiple joints constrained to act as a unit. For example, when the orientation of the hand is not externally constrained by the object's geometry (reaching for a ball or just pointing at it) there should be little need for control of the forearm orientation. This may be the case in our study. Therefore, we have found that the upper arm (as compared to the forearm) complied more with Donders' and Listing's laws. However, during other tasks the brain may couple the arm joints to act as a unit under the constraint of Listing's law (Marotta et al. 2003).

If a thick two-dimensional surface indeed constrains the rotations of the upper arm segment within reasonable margins of error as is suggested by our results, the extrinsic kinematics of the hand could be predicted using a flat Listing's plane on the shoulder as a simplifying assumption. This would require additional assumptions regarding the path and the temporal evolution of the rotation vectors of the shoulder within the plane, and a description of the relationship between the rotations of the elbow with respect to the rotations of the shoulder.

In a sense, the present findings provide a guideline and a motive for the implementation of Listing's law as a constraint in a modeling approach that is developed in the accompanying manuscript.

References

Admiraal MA, Medendorp WP, Gielen CCAM (2001) Three-dimensional head and upper arm orientations during kinematically redundant movements and at rest. Exp Brain Res 142:181–192

Bernstein N (1967) The coordination and regulation of movements. Pergamon Press, Oxford

Ceylan M, Henriques DYP, Tweed DB, Crawford JD (2000) Task-dependent constraints in motor control: pinhole goggles make the head move like an eye. J Neurosci 20:2719–2730

Crawford JD, Vilis T (1995) How do motor systems deal with the problems of controlling three-dimensional rotations? J Mot Behav 27:89–99

DeSouza JFX, Nicolle DA, Vilis T (1997) Task-dependent changes in the shape and thickness of Listing's plane. Vision Res 37:2271–2282

Donders FC (1847) Beitrag zur Lehre von den Bewegungen des menschlichen Auges. Holländ Beitr Anat Physiol Wiss 1:104–145

Gielen CCAM, Vrijenhoek EJ, Flash T, Neggers SFW (1997) Arm position constraints during pointing and reaching in 3D. J Neurophysiol 78:1179–1196

Glenn B, Vilis T (1992) Violations of Listing's law after large eye and head gaze shifts. J Neurophysiol 68:309–318

Haslwanter T (1995) Mathematics of 3-dimensional eye rotations. Vision Res 35:1727–1739

Hepp K (1990) On Listing's law. Commun Math Phys 132:285–292

Hollerbach JM, Flash T (1982) Dynamic interactions between limb segments during planar arm movement. Biol Cybern 44:67–77

Hore J, Watts S, Vilis T (1992) Constraints on arm position when pointing in three dimensions: Donders' law and the Fick-gimbal strategy. J Neurophysiol 68:374–383

Marotta JJ, Medendorp WP, Crawford JD (2003) Kinematic rules for upper and lower arm contributions to grasp orientation. J Neurophysiol 90:3816–3827

Medendorp WP, Van Gisbergen JAM, Horstink MWIM, Gielen CCAM (1999) Donders' law in Torticollis. J Neurophysiol 82:2833–2838

Medendorp WP, Crawford JD, Henriques DYP, Van Gisbergen JAM, Gielen CCAM (2000) Kinematic strategies for upper arm–forearm coordination in three dimensions. J Neurophysiol 84:2302–2816

Miller LE, Theeuwen M, Gielen CCAM (1992) The control of arm pointing movements in three dimensions. Exp Brain Res 90:415–426

Mitra S, Turvey MT (2004) A rotation invariant in 3-D reaching. J Exp Psychol Hum Percept Perform 30:163–169

Morasso P (1981) Spatial control of arm movements. Exp Brain Res 42:223–227

Van Opstal J (1993) Representation of eye position in three dimensions. In: Berthoz A (ed) Multi-sensory control of movement. Oxford University Press, Oxford, pp 27–41

Soechting JF, Buneo CA, Herrmann U, Flanders M (1995) Moving effortlessly on three dimensions: does Donders' law apply to arm movements? J Neurosci 15:6271–6280

Straumann D, Haslwanter T, Hepp-Reymond MC, Hepp K (1991) Listing's law for the eye, head and arm movements and their synergistic control. Exp Brain Res 86:209–215

Theeuwen M, Miller LE, Gielen CCAM (1993) Are the orientations of the head and arm related during pointing movements? J Mot Behav 25:242–250

Tweed D (1999) Three-dimensional model of the human eye–head saccadic system. J Neurophysiol 77:654–666

Tweed D, Vilis T (1987) Implications of rotational kinematics for the oculomotor systems in three dimensions. J Neurophysiol 58:832–849

Tweed D, Vilis T (1990) Geometric relations of eye position and velocity vectors during saccades. Vision Res 30:111–127

Westheimer G (1957) Kinematics of the eye. J Optic Soc Am 47:967–974